Power losses in a suspension of magnetic dipoles under a rotating field

Yu. L. Raikher and V. I. Stepanov
Institute of Continuous Media Mechanics, Ural Branch of Russian Academy of Sciences, Perm RU-614013, Russia
(Received 1 September 2010; published 14 February 2011)

Energy absorption due to viscous friction in a dilute suspension of single-domain ferromagnetic particles subjected to a rotating field is considered. The problem is treated in the framework of kinetic approach. The behavior of specific loss power (SLP) as a function of the field amplitude and frequency is studied. It is shown that for either of these parameters (while the other is kept constant) SLP first grows quadratically and then saturates. The cases of a rotating field and oscillating fields are compared, and the essential differences are revealed. The results obtained enable one to assess the allowable or optimal field parameters for a given magnetic suspension intended for rotational magneto-inductive heating.

DOI: 10.1103/PhysRevE.83.021401 PACS number(s): 83.80.Hj, 47.65.Cb, 75.50.Mm, 75.60.Ej

I. INTRODUCTION

Theory of the magneto-inductive hyperthermia (MIH) is rapidly developing nowadays. It is natural that, as the technique becomes closer to practical use, the theory specializes. The set of concepts and models, increasing in number, separates into trends, which differ in essential details: the use of either superparamagnetic or magnetically rigid particles, heat generation in either highly or low viscous or viscoelastic media, etc. On the other hand, the principal criterion for any MIH method or its modification is the specific loss power (SLP) attained. Conventionally, the value of this parameter is determined with respect to a unit mass of a ferrite or ferromagnet particles, which are the MIH mediators, i.e., microgenerators of heat. An important aspect of the MIH technique is the type of field acting on the particles embedded into the object intended for heating. As the literature shows, in the overpowering majority of laboratory and practical experiments the inductor is a single solenoid generating a uniform linearly polarized alternating field (AC) [1–7]. Accordingly, this configuration is adopted in theoretical modeling of magneto-inductive heating, see Refs. [2,8,9], for example. Meanwhile, since very recently an interest to heat generation under a rotating field has emerged because of promising estimates of the attainable SLP; see Ref. [10], where an experiment of such a kind is reported. The goal of the present paper is to show that the theory of MIH with a rotating field has some unique features and by no means is exhausted by a simple doubling of the acting field strength.

The key point for investigation of the effect of a rotating field on a magnetic suspension (magnetic fluid) is the equation of motion for magnetization of the system. Its derivation requires a mesoscopic consideration: one needs to solve the problem of rotation of a magnetic Brownian particle in a viscous fluid.[1] This issue was addressed many times from both phenomenological [13,14] and kinetic [15–17] positions. However, until now the solutions obtained were aimed at and used mostly for investigations of either the magnetoviscous effect or the induction of magnetic fluid hydrodynamic flows. As a result, heat generation under a rotating field and the dependencies of the energy absorption on the main field and particle parameters were not consistently studied whatsoever. In the present paper, on the basis of a kinetic model we analyze the response of a dilute assembly of magnetically rigid Brownian particles, suspended in a fluid, to a rotating magnetic field and analyze the behavior of SLP with respect to field amplitude and frequency and to temperature. Special attention is given to the limit of "large" particles, viz. the situation, where the Brownian motion is vanishingly small. This case is important both fundamentally and practically in view of numerous laboratory experiments where the particles more coarse than those of magnetic fluids are employed [2,4].

[1]As follows from the hydrodynamics of magnetic fluid under rotating field [11,12], if the fluid in a vessel does not have free surfaces, no macroscopic rotation is induced.

II. THEORETICAL MODEL

Consider a magnetic suspension that is dilute to such an extent that the single-domain particles residing therein might be treated as independent. Then the problem of MIH reduces to the one of heat generation in a statistical ensemble of noninteracting particles suspended in a quiescent linearly viscous medium. The orientation-dependent part of the energy that each particle acquires under an external field $\boldsymbol{H}$ is

$$U = -\mu H(\boldsymbol{e} \cdot \boldsymbol{h}), \tag{1}$$

where $\mu = M_S V_m$ is the magnetic moment, V_m the volume of the particle magnetic "core," and M_S the ferromagnet magnetization. The magnetic anisotropy (magnetic rigidity) of the particle is assumed to be sufficiently high, so that the magnetic moment is always aligned with the easy magnetization axis, i.e., the particle is in fact a nanosize permanent magnet. Due to that, a unit vector $\boldsymbol{e}$ in Eq. (1) denotes, equivalently, both the direction of the particle magnetic moment and the direction of the particle geometry axis. We define the laboratory coordinate frame by superimposing its plane with the plane of rotation of the field $\boldsymbol{H}$, so that a unit vector has the components

$$\boldsymbol{h} = (\cos \omega t, \sin \omega t, 0), \tag{2}$$

with ω being the frequency of the field rotation; as seen, the field (2) is right-handedly circularly polarized. To obtain a steady solution, it is convenient to pass from the laboratory frame to the one rotating with the field; this is done by setting $\phi = \varphi - \omega t$. In this representation the major vectors of the problem expressed in terms of spherical coordinates (the polar axis is normal to the field rotation plane) are

$$\boldsymbol{h} = (1,0,0), \quad \boldsymbol{e} = (\sin\theta\cos\phi, \sin\theta\sin\phi, \cos\theta), \tag{3}$$

while the particle energy (1) takes the form

$$U = -\mu H \sin\theta\cos\phi, \tag{4}$$

which does not explicitly depend on time.

For nanosize particles, Brownian motion is an essential factor. An ensemble of such particles, provided their interactions are negligible, is described by a single-particle distribution function $W(\boldsymbol{e},t)$ that obeys the orientational diffusion (Fokker-Planck) equation, see [18], for example. In the rotating frame, this equation takes the form

$$2\tau_B[\partial/\partial t - (\boldsymbol{\omega}\hat{\boldsymbol{J}})]W = \hat{\boldsymbol{J}}W\hat{\boldsymbol{J}}(U/k_BT + \ln W), \tag{5}$$

where $\hat{\boldsymbol{J}} = \boldsymbol{e}\times\partial/\partial\boldsymbol{e}$ is the infinitesimal rotation operator, $\tau_B = 3\eta V_h/kT_B$ is the timescale of Brownian rotary diffusion, η the fluid viscosity, and V_h the "hydrodynamic" volume of the particle that allows for the presence of a nonmagnetic surface layer and an outer (surfactant or other) shell. When the system attains a steady state, the time derivative in Eq. (5) becomes zero.

The dimensionless parameters of the problem are introduced as follows:

$$\tau_B = \tau_0\xi, \quad \tau_0 = 3\eta V_h/\mu H, \quad \xi = \mu H/k_BT, \tag{6}$$

and steady distribution function is presented in the form of a series

$$W(\theta,\phi) = \sum_{l=0}^{\infty}\sum_{k=-l}^{k=l} b_{l,k}Y_{l,k}(\theta,\phi), \tag{7}$$

with respect to normalized spherical harmonics $Y_{l,k}$ defined as

$$Y_{l,k}(\theta,\phi) = (-1)^k\sqrt{\frac{(2l+1)(l-k)!}{4\pi(l+k)!}}P_l^k(\cos\theta)e^{ik\phi}; \quad -l \leqslant k \leqslant l, \quad Y_{l,k}^* = (-1)^kY_{l,-k}. \tag{8}$$

Substitution of Eq. (7) in (5) with allowance for Eq. (8), renders an infinite chain of two-index recurrence equations

$$-2ik\omega\tau_B b_{l,k} + l(l+1)b_{l,k} = \frac{\xi}{2}\left[(l+1)\sqrt{\frac{(l-k-1)(l-k)}{(2l-1)(2l+1)}}b_{l-1,k+1} + l\sqrt{\frac{(l+k+2)(l+k+1)}{(2l+1)(2l+3)}}b_{l+1,k+1} - (l+1)\sqrt{\frac{(l+k-1)(l+k)}{(2l-1)(2l+1)}}b_{l-1,k-1} - l\sqrt{\frac{(l-k+2)(l-k+1)}{(2l+1)(2l+3)}}b_{l+1,k-1}\right], \tag{9}$$

that is convenient to solve with the aid of matrix sweeping method [19]. For the problem under study, the issue of prime interest is the coefficient $b_{1,1}$ because it defines the projection of the ensemble magnetization onto the plane of rotation of the field. In a normalized form, this two-dimensional vector is expressed in terms of $b_{1,1}$ as

$$\boldsymbol{m} = (m_\parallel, m_\perp), \quad m_\parallel = \langle\sin\theta\cos\phi\rangle = -\sqrt{\frac{8\pi}{3}}\mathrm{Re}b_{1,1}, \quad m_\perp = \langle\sin\theta\sin\phi\rangle = \sqrt{\frac{8\pi}{3}}\mathrm{Im}b_{1,1}, \tag{10}$$

where subscripts indicate the directions with respect to vector $\boldsymbol{h}$ and angular brackets denote the statistical ensemble averaging. There are two main cases, when the kinetic equation (5) has analytical solutions. Assuming $\xi \ll 1$ (low field amplitudes and/or high temperatures) and retaining in Eq. (9) the harmonics with $l \leqslant 1$, one finds

$$m = m_\parallel - im_\perp = \frac{\xi}{3}\frac{1}{1+i\omega\tau_B}; \tag{11}$$

evidently, for a field rotating in opposite direction, Eq. (11) should be replaced by its complex conjugate. In the athermal limit (vanishing Brownian motion, $\xi\to\infty$) the dynamics of the particle is determined by the combined action of the viscous and magnetic torques and is described by a set of equations

$$\frac{\partial\phi}{\partial t} = \omega - \frac{1}{2\tau_0}\frac{\sin\phi}{\sin\theta}, \quad \frac{\partial\theta}{\partial t} = \frac{1}{2\tau_0}\cos\theta\cos\phi. \tag{12}$$

When the low-frequency condition $2\omega\tau_0 < 1$ holds, the steady $(\partial/\partial t = 0)$ solution takes the form

$$\theta = \tfrac{1}{2}\pi, \quad \phi = \arcsin(2\omega\tau_0). \tag{13}$$

In this regime, the normalized magnetization takes the form

$$m_\parallel = \sqrt{1-4\omega^2\tau_0^2}, \quad m_\perp = 2\omega\tau_0 \tag{14}$$

evidencing that in the rotating frame vector $\boldsymbol{m}$ remains constant and is tilted to the direction of the field under the angle ϕ defined by Eq. (13). In the case of high frequencies the particle magnetic moment may assume any of the accessible variety of orbits, all of which are isochronous. The period of the occurring precession differs from that of the field and equals [20,21]

$$T = \frac{2\pi\tau_0}{\sqrt{(2\omega\tau_0)^2-1}}. \tag{15}$$

A first asymptotic $(\xi\to\infty)$ solution for $\boldsymbol{m}$ was given in Ref. [20]. There the authors determined the ensemble magnetization by averaging over the period (15) and assuming that all the magnetic moment orbits are equiprobable. As it was shown later by Hinch and Leal [21], this conjecture holds only for the time intervals shorter than τ_B, when the system had not yet "forgotten" completely the initial conditions. Due to this reason, the solution given in [20] is not entirely steady. In Ref. [21] it is found that in the true steady state of the athermal limit the distribution of the magnetic moments over the set of orbits is nonuniform. The authors obtained a solution for $t \to \infty$ by imposing a requirement that the flux density of the representing points at the surface of a unit sphere turns to zero in the direction normal to the "orbital" motion of vector $\boldsymbol{e}$. In our notations (6) and (10), the components of vector $\boldsymbol{m}$ found in [21] are

$$m_\parallel = 0, \quad m_\perp = 2\omega\tau_0 - \frac{4\omega^2\tau_0^2 - 1}{2\sqrt{3}\omega\tau_0} \ln\left(\frac{\sqrt{8\omega^2\tau_0^2+1}+\sqrt{3}}{\sqrt{8\omega^2\tau_0^2+1}-\sqrt{3}}\right)\left[\ln\left(\frac{\sqrt{8\omega^2\tau_0^2+1}+1}{\sqrt{8\omega^2\tau_0^2+1}-1}\right)\right]^{-1}. \tag{16}$$

In the high-frequency limit $m_\perp$ can be expanded in the asymptotic series

$$m_\perp = \frac{1}{3}\frac{1}{\omega\tau_0} + \frac{7}{360}\frac{1}{(\omega\tau_0)^3} + \frac{23}{15120}\frac{1}{(\omega\tau_0)^5} + \cdots, \tag{17}$$

whose first term coincides with the high-frequency limit of Eq. (11).

In Fig. 1 the transverse magnetization $m_\perp$ evaluated numerically with the aid of Eq. (9) is presented for several reference values of ξ. As seen, all the lines corresponding to finite temperatures lie inside the limiting contour formed by the athermal low-frequency (14) and high-frequency (16) branches, which meet at $\omega\tau_0 = 1/2$. The ascending (low-frequency) parts of all the plots have initial linear behavior, whose tangent for any value of ξ can be written in the form

$$m_\perp/\omega = \tau_\perp L(\xi), \tag{18}$$

where $L(\xi)$ is Langevin function and $\tau_\perp$ is the relaxation time of the normal to the field magnetization component determined under a constant ($\omega = 0$) field. A full numeric evaluation of $\tau_\perp$ is given in Ref. [22], where it is denoted as $\tau_{\rm eff}^{(1)}$. In the same work it is shown that in the entire ξ range the exact $\tau_\perp$ with good accuracy is reproduced by a simple expression

$$\tau_\perp = \frac{2\xi L}{\xi - L}\tau_0, \tag{19}$$

obtained in Ref. [23] in a so-called effective-field approximation. As is easy to see, the relaxation time (19) changes from $\xi\tau_0 = \tau_B$ at $\xi \ll 1$ (high temperatures) to $2\tau_0$ at $\xi \to \infty$ (low temperatures). In the latter case, formula (18) reduces to the afore-obtained athermal limiting value (14) for $m_\perp$. With expression (19) the tangents of the curves in Fig. 1 are given by

$$m_\perp/\omega\tau_0 = \frac{2\xi L^2(\xi)}{\xi - L} = \begin{cases} \frac{1}{3}\xi^2 & \text{for } \xi \ll 1, \\ 2 - 2/\xi & \text{for } \xi \gg 1. \end{cases} \tag{20}$$

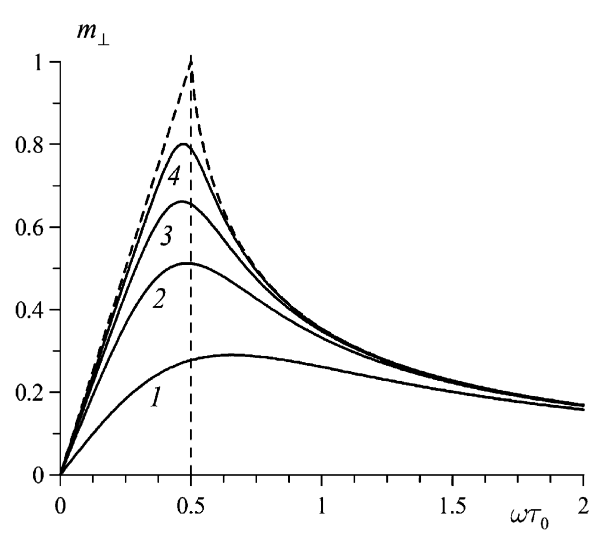

FIG. 1. Frequency dependence of the transversal magnetization for the rotating field amplitudes $\xi = 2$ (*1*), 5 (*2*), 10 (*3*), 25 (*4*), and the athermal limit $\xi = \infty$ (dashed).

III. ENERGY ABSORPTION

The viscous torque acting on a field-driven rotating particle causes its magnetic moment to lag behind the field. The lag angle between vectors $\boldsymbol{e}$ and $\boldsymbol{H}$ is directly connected to the dissipation that accompanies this motion. Indeed, the heat generation by one particle (the work of viscous forces) per cycle of the field is given by formula

$$A = \mu \oint (\boldsymbol{e}\cdot d\boldsymbol{H}) = \mu \int_0^{2\pi/\omega} (\boldsymbol{e}\cdot\dot{\boldsymbol{H}})dt; \tag{21}$$

note that in a nonconducing suspension of magnetically rigid particles this viscous dissipation is the only source of heating.

To evaluate integral (21), we get back to the laboratory frame, where the components of unit vectors $\boldsymbol{e}$ and $\boldsymbol{h}$ explicitly depend on time. After integration over the rotation period $2\pi/\omega$ one gets

$$A = 2\pi\mu H\langle\sin\theta\sin\phi\rangle = 2\pi\mu H m_\perp. \tag{22}$$

As mentioned above, the specific-loss power is defined per unit mass of the particle. Using formula (22), one finds

$$\mathrm{SLP} = \frac{\omega A}{2\pi\rho V_m} = \frac{1}{\rho}\omega M_S H m_\perp; \tag{23}$$

here ρ is the specific-mass density of the particle. In below, it is convenient to rescale SLP according to the relation

$$\mathcal{S} = \frac{\rho V_m \tau_B}{k_B T} \times (\mathrm{SLP}) = \xi\omega\tau_B m_\perp, \tag{24}$$

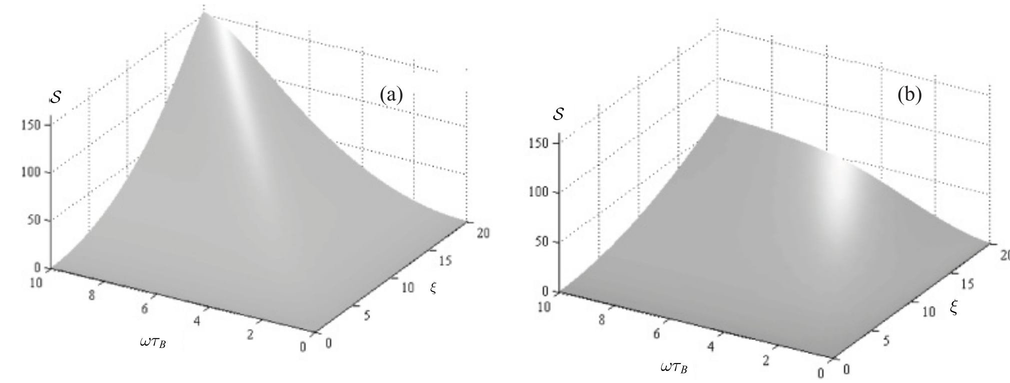

FIG. 2. Specific loss power for rotating (a) and oscillating (b) fields; function $\mathcal{S}$ is normalized according to Eq. (24).

and express it as a function of the dimensionless parameters ξ and $\omega\tau_B$. The advantage is that with this choice the field and frequency arguments of $\mathcal{S}$ are independent under isothermal conditions; the variable $\omega\tau_0$ employed in Fig. 1 is convenient only for the analysis with respect to the athermal limit.

The above-obtained approximations for $m_\perp$ readily deliver the behavior of $\mathcal{S}$ in two important asymptotic cases. Namely, for $\omega\tau_B/\xi \gg 1$, that means low fields and/or high frequencies, from Eq. (17) one gets

$$\mathcal{S} = \frac{1}{3}\xi^2 + \frac{7}{360}\frac{\xi^4}{(\omega\tau_B)^2} + \frac{23}{15120}\frac{\xi^6}{(\omega\tau_B)^4} + \cdots . \quad (25)$$

Therefore, in the $\omega\tau_B \to \infty$ limit SLP saturates with respect to the frequency and scales quadratically with the field.

In the opposite case $\omega\tau_B/\xi < 1/2$, i.e., strong fields and/or low frequencies, Eq. (20) renders

$$\mathcal{S} = 2\omega^2\tau_B^2 \frac{\xi L^2(\xi)}{\xi - L(\xi)} \simeq 2\omega^2\tau_B^2\left(1 - \frac{1}{\xi}\right) \quad (26)$$

indicating that SLP saturates with respect to the field amplitude and is quadratic in the frequency parameter.

IV. DISCUSSION

In view of the MIH applications, the issue of prime interest is to compare the obtained SLP dependencies for a rotating field with those for an oscillating one. The overall shapes of the surfaces $\mathcal{S}(\xi,\omega\tau_B)$ for these field configurations are shown in Fig. 2; the surface in Fig. 2(b) presents the one given in Ref. [9] transformed from the $\omega\tau_0$ to $\omega\tau_B$ coordinate.

A distinctive feature of the surface $\mathcal{S}(\xi,\omega\tau_B)$ for a rotating field is a rather sharp edge "hovering" over the straight line $\omega\tau_B = \xi/2$. The latter maps the position of the summit point of Fig. 1 to the coordinates of Fig. 2. This straight line divides the plane of parameters $(\xi,\omega\tau_B)$ in two parts. In the weak field region ($\xi < 2/\omega\tau_B$) the function $\mathcal{S}(\xi)$ at any frequency first grows quadratically with the field and then, after having traversed the edge, saturates. Equation (25), where all the terms are positive, indicates a specific limiting behavior of the function $\mathcal{S}(\xi,\omega\tau_B)$. Namely, it approaches the saturation level from above thus establishing that at high frequencies the function passes a weak maximum.

On the other side of the border, i.e., in the $\xi > 2\omega\tau_B$ half-plane, similar behavior is displayed by the function $\mathcal{S}(\omega\tau_B)$: at any ξ it increases quadratically before attaining the edge but ceases to grow after having crossed it, see Eq. (26). Note that here, i.e., with respect to the frequency, the function $\mathcal{S}$ saturates monotonically.

All the above-mentioned features of SLP are clearly visible in Fig. 3, where the exact (obtained from the numeric solution) cross sections of the surface of Fig. 2(a) by the planes $\omega\tau_B = \text{const}$ and $\xi = \text{const}$ are presented. One can see that the functions $\mathcal{S}(\xi)|_{\omega\tau_B}$ and $\mathcal{S}(\omega\tau_B)|_\xi$, after having traversed the edge, flatten the stronger, the greater is the value of the argument that is kept constant. Comparison with the analog logarithmic plots for the oscillating field case shown in Fig. 4 reveals that the main difference is in the field-parameter behavior of SLP. Function $\mathcal{S}(\xi)$ that saturates with ξ under a rotating field, under an oscillating one only changes the rate of its growth: from quadratic to linear, see Ref. [9].

Figure 2, compared in general, shows that, as expected, at large values of the principal arguments the SLP in a rotating field is about twice as high as that in an oscillating field. However, for accurate comparison, cross sections are much more instructive. In Fig. 5 the respective SLP functions for two reference values of ξ are presented. In particular, this plot allows one to clearly distinguish the region of the high-frequency maximum of SLP, whose existence follows from the

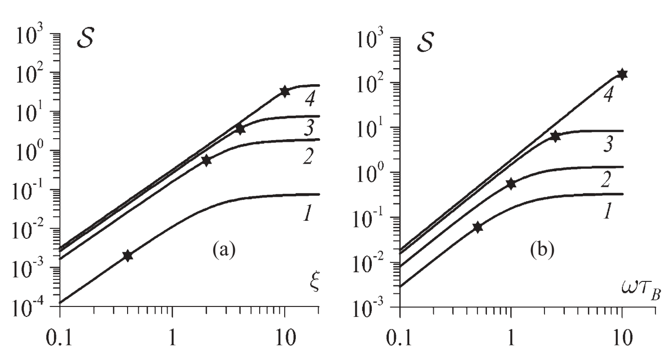

FIG. 3. Specific loss power in a rotating field as a function of (a) magnetic field strength for $\omega\tau_0 = 0.2$ (*1*), 1 (*2*), 2 (*3*), 5 (*4*) and (b) field rotation frequency for $\xi = 2$ (*1*), 5 (*2*), 10 (*3*), 20 (*4*); in both panes the asterisks mark the points corresponding to the condition $\omega\tau_0 = 1/2$.

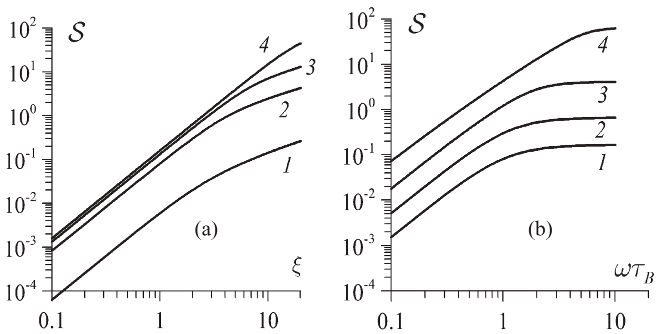

FIG. 4. Specific loss power in an oscillating field as a function of (a) magnetic field strength for $\omega\tau_0 = 0.2$ (*1*), 1 (*2*), 2 (*3*), 5 (*4*) and (b) field rotation frequency $\xi = 2$ (*1*), 5 (*2*), 10 (*3*), 20 (*4*).

form of the asymptotic expansion (25). A notable circumstance is that, in contrary to the general prediction, at low frequencies and strong fields the oscillating field is as good as the rotating one and even better, see Fig. 5(b).

To clarify the occurrence of such a crossover between the rotating and oscillating field SLP's, we compare the respective functions $\mathcal{S}$ by plotting them in Fig. 6 as functions of the parameter $\omega\tau_0$. One can see that in the $\xi = \infty$ limit, with the decrease of $\omega\tau_0$ the AC curve ascends, crosses that for the rotating field and grows monotonically until $\omega\tau_0 = 0$; the crossing point is $\omega\tau_0 = 0.245$. For lower frequencies/stronger fields the absorption in an AC field is more efficient, while for higher frequencies/weaker fields a rotating field heats better that an AC one. To the right of the summit point, that is for $\omega\tau_0 > 1/2$, both lines descend coherently, the ratio between their heat effects being 2 : 1. As seen from Fig. 6 for finite ξ's the situation is qualitatively the same, i.e., in the low-frequency region AC becomes more efficient. The only difference is that, as the absorption is proportional to the out-of-phase part of the magnetic response, both SLP curves tend to zero at $\omega\tau_0 = 0$.

We remark one formal circumstance related to the dashed curve *2* (the athermal limit for the oscillating field case) in Fig. 6. It is well known that in calculations of the dissipation per cycle (dynamic hysteresis) the limits $\xi = \infty$ ($T = 0$) and $\omega = 0$ are noncommutative. In our case this means that if to plot A as a function of the formal argument ($\omega\tau_0$) increasing ξ unboundedly but keeping $\omega \neq 0$, this sequence would finish

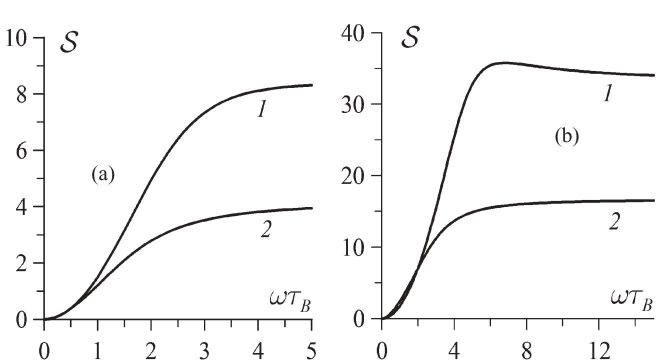

FIG. 5. Comparison of specific loss power vs frequency for rotating (curves *1*) and oscillating (curves *2*) fields at $\xi = 5$ (a) and 10 (b).

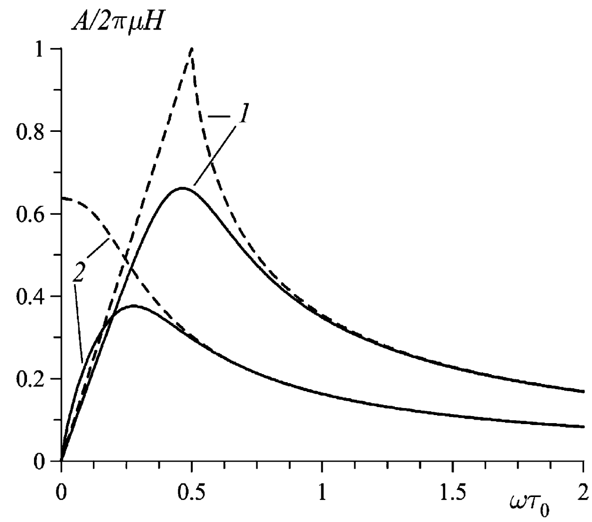

FIG. 6. Energy absorption per cycle for a particle subjected to a rotating (*1*) or oscillating (*2*) field; values of the field strength parameter ξ are ∞ (dashed) and 10 (solid).

with a curve, which abuts on the ordinate axis at the value $2/\pi$. On the other hand, if to perform the same calculation of A decreasing ω to zero but keeping $\xi \neq 0$, the final curve of this sequence would come up to a maximum (that may be arbitrarily close to the point $\omega\tau_0 = 0$ in its position and to $2/\pi$ in its value) but after that would fall down vertically to zero. Therefore, for any $\omega\tau_0 \neq 0$ the curves of both types coincide differing only in the infinitesimal vicinity of the limiting point. This peculiarity of the function A, being important mathematically, could hardly affect any real situation.

The developed model of energy absorption under a rotating field is based on the assumption that the medium, which the field works on, is nonconducting. Therefore, the condition of its validity is a requirement that the magneto-inductive thermal effect is greater than that of nonspecific "eddy current" heating. The order of magnitude of the latter is $\sigma(\omega H D/c_0)^2$, where σ is conductivity, D the spatial scale of the field, i.e., the dimension of the induction zone, and c_0 the velocity of light. Comparing volumetric densities of the magnetic and eddy current losses, one arrives at the restriction

$$fH < \frac{n\mu m_\perp}{2\pi\sigma}\left(\frac{c_0}{D}\right)^2, \tag{27}$$

where $f = \omega/2\pi$ is cyclic frequency and n is the number concentration of the ferromagnetic particles. For the regime of maximal magnetic heating ($\omega\tau_B = \xi/2$) one should replace $m_\perp$ in Eq. (27) by unity. Equivalently, in this regime a possibility to neglect the eddy current effect is expressed by either of the inequalities

$$H < \frac{c_0}{D}\sqrt{\frac{6n\eta V_h}{\sigma}}, \quad f < \frac{c_0\mu}{2\pi D}\sqrt{\frac{n}{6\sigma\eta V_h}} \tag{28}$$

depending on what quantity is estimated.

Let us consider, as an example, a magnetic suspension with volume fraction $\phi = 10\%$ of ferrite ($M_S = 400$ G) particles so that the saturation magnetization is $\phi M_s \sim 40$ G. Assuming $\sigma \sim 6 \times 10^9$ CGS = 0.7 S/m for the conductivity of the carrier fluid (human blood at temperature 37 °C [24]) and $D = 30$ cm for the induction zone size, from Eq. (27) one gets $fH < 10^9$ Hz Oe $= 8 \times 10^{10}$ Hz A/m. For a typical excitation frequency $f \sim 100$ kHz, this yields $H < 10^4$ Oe. Since the field amplitudes, which are really attainable in the given frequency range, are at least an order of magnitude lower, this estimate ensures a minor role of eddy current losses.

For medical applications of alternating magnetic fields there exists an empiric restriction that defines physiologically acceptable fH level. This bound is called Brezovich's rule and, as described in Ref. [25], for $D = 30$ cm it gives

$$fH < C, \quad C \simeq 6 \times 10^6 \text{ Hz Oe} = 5 \times 10^8 \text{ Hz A/m}. \tag{29}$$

Unlike Eq. (27) this expression is insensitive to the presence/absence of ferromagnetic particles in the heated tissue. Because of that, Brezovich's rule is an independent restriction on any MIH model. Comparing the numerical estimates of the right-hand parts of Eqs. (27) and (29) for the above-considered example, one finds that Brezovich's restriction is about two orders of magnitude stronger. Due to that, the field range allowable for medical MIH ought to be estimated from Eq. (29). Choosing again the optimal heating regime $\omega\tau_B = \xi/2$ and substituting this relation in Eq. (29), one gets

$$H \lesssim \sqrt{\frac{12\pi\eta C}{M_S}\frac{V_h}{V_m}}, \tag{30}$$

cf. Eq. (28). Setting $V_h/V_m \sim 10$ and $\eta \sim 10^{-2}$ Ps, one gets from Eq. (30) quite a reasonable estimate $H \lesssim 250$ Oe $\simeq$ 20 kA/m. Transforming this to determine the frequency, one finds $f \sim 20$ kHz. Thus we see that the obtained optimal field and frequency values fall well within the parameter ranges, where MIH is performed [1–7].

As it follows from the presented results, to make the magnetic heating more intense and frequency-sensitive, one has to have the particle Langevin parameter considerably greater than unity. To attain $\xi \gtrsim 5$ at room temperature and in a field of amplitude $H \sim 100$ Oe, one needs the ferrite particles of diameter ∼20–25 nm, which estimate agree well, for example, with the recommendations of Ref. [3], where oscillating-field MIH was discussed.

Finally, we remark on the validity of the dilute system approximation that we use. Apparently, the greater the particles, the more probable is their aggregation due to the dipole-dipole interactions. As the simulations reported in Ref. [26] have revealed,[2] under a rotating field a suspension of permanent dipoles might split into well-separated flat monolayers of the particles in the direction normal to the field plane. In the occurring structure the layers repel each other, while inside each layer the particle distribution is gas-like, i.e., resembling that of a dilute system. The examples given in [26] show that this "phase separation" takes place for $\xi = 14$ (and larger) at the particle volume fraction 10 vol.% and higher. This implies that for lower field parameters, e.g., $\xi = 5$, the dilute system limit should hold at leat up to 10 vol.%.

[2]We are grateful to the referee of our paper for bringing this paper to our attention.

V. CONCLUSIONS

Specific loss power for a dilute suspensions of magnetic dipole particles in a viscous fluid is given, and the SLP dependencies on the frequency and amplitude of a rotating field are analyzed under isothermal conditions. The condition of maximal absorption with plausible accuracy is given by the relation $\omega\tau_B = \xi/2$. Being transformed back to dimensional units, it enables one to assess the optimal ranges for real parameters of rotational magneto-inductive heating on the basis of the following simple rules:

(i) under fixed frequency of rotation the absorbed power grows quadratically with field amplitude and attains a virtually maximal value at $H_* \simeq 6\omega\eta V_h/M_S V_m$; any further increase of H is inefficient;

(ii) under fixed amplitude of the field the absorbed power grows quadratically with field frequency and attains a virtually maximal value at $\omega_* \simeq M_S H V_m/6\eta V_h$; any further increase of ω is inefficient.

The above-given estimates do not contain temperature explicitly, and as such are appropriate mostly for the high-field/massive-particle case. More accurate considerations bring in the thermal effect, which is the greater the higher the temperature of the system. For example, as follows from Fig. 3, at $\omega\tau_B = 0.2$ the quadratic behavior of SLP still holds for the fields, which exceed H_* by almost an order of magnitude. Similar underestimation one encounters for ω_* as well, see in Fig. 3(b) the curve corresponding to $\xi = 2$ that is the lowest of the values presented. However, the mentioned deviations reduce rapidly with the temperature decrease.

Comparison with the conventional case—linearly polarized oscillating field—reveals a number of differences between the field and frequency behaviors of heating. These differences are caused by a specific mechanism inherent to the rotary motion of a particle: dynamic crossover between the synchronous and asynchronous regimes. The transition from one regime to another can be induced, for example, by increasing the field amplitude while keeping the frequency constant. In the crossover point the system energy dissipation (absorption) is maximal. Moreover, in the crossover region the rotational magnetic heating is substantially more efficient and has higher frequency selectivity than oscillatory heating. This domination is not universal, however. Under off-maximum conditions there is a sufficiently wide parameter domain (low frequency and/or strong field), where the rotational absorption is lower than that induced by an oscillating field of the same amplitude and frequency. This is one of manifestations of a fundamental difference between the asymptotic field dependencies of SLP: saturation for the rotation case and linear increase for the oscillation one, cf. Figs. 3(a) and 4(a).

ACKNOWLEDGMENTS

The work was done under auspices of the projects: RFBR 08-02-00802, RFBR-CNRS 09-02-91070 (PICS 4825), and ECONET 21394NH. Authors are grateful to V. A. Sharapova, A. E. Yermakov, M. A. Uymin, and V. V. Rusakov for useful discussions.

[1] R. Hergt, R. Hiergeist, M. Zeisberger, G. Glockl, W. Weitschies, L. P. Ramirez, I. Hilger, and W. A. Kaiser, J. Magn. Magn. Mater. **280**, 358 (2004).
[2] J.-P. Fortin, J. Servais, C. Wilhelm, C. Menager, J.-C. Bacri, and F. Gazeau, J. Am. Chem. Soc. **129**, 2628 (2007).
[3] J.-P. Fortin, F. Gazeau, and C. Wilhelm, Eur. Biophys. J. **37**, 223 (2008).
[4] B. E. Kashevsky, V. E. Agabekov, S. B. Kashevsky, K. A. Kekalo, E. Y. Manina, I. V. Prokhorov, and V. S. Ulashchik, Particuology **6**, 322 (2008).
[5] L. M. Lacroix, R. B. Malaki, J. Carrey, S. Lachaize, M. Respaud, G. F. Goya, and B. Chaudret, J. Appl. Phys. **105**, 023911 (2009).
[6] E. Duguet, L. Hardel, and S. Vasseur, *Cell Targeting and Magnetically Induced Hyperthermia*, Topics in Applied Physics, Vol. 118 (Springer-Verlag, Berlin/Heidelberg, 2009), Chap. 11, pp. 343–365.
[7] M. Winkler, A. Kaiser, S. Krause, H. Finkelmann, and A. M. Schmidt, Macromol. Symp. **291–292**, 186 (2010).
[8] R. E. Rosensweig, J. Magn. Magn. Mater. **252**, 370 (2002).
[9] Y. L. Raikher and V. I. Stepanov, J. Magn. Magn. Mater. **320**, 2692 (2008).
[10] V. A. Sharapova, M. A. Uymin, A. A. Mysik, and A. E. Yermakov, Phys. Met. Metallogr. **110**, 5 (2010).
[11] R. E. Rosensweig, J. Popplewell, and R. J. Jonston, J. Magn. Magn. Mater. **85**, 171 (1990).
[12] A. V. Lebedev and A. F. Pshenichnikov, J. Magn. Magn. Mater. **122**, 227 (1993).
[13] M. I. Shliomis, Sov. Phys. JETP **34**, 1291 (1972).
[14] M. I. Shliomis, Sov. Phys. Dokl. **19**, 686 (1975).
[15] A. C. Levi, R. F. Hobson, and F. R. McCourt, Can. J. Phys. **51**, 180 (1973).
[16] M. I. Shliomis, T. P. Lyubimova, and D. V. Lyubimov, Chem. Eng. Comm. **67**, 275 (1988).
[17] B. U. Felderhof, Phys. Rev. E **66**, 051503 (2002).
[18] Y. L. Raikher and M. I. Shliomis, Adv. Chem. Phys. **87**, 595 (1994).
[19] Y. L. Raikher and V. I. Stepanov, Adv. Chem. Phys. **129**, 419 (2004).
[20] W. F. Hall and S. N. Busenberg, J. Chem. Phys. **51**, 137 (1969).
[21] E. J. Hinch and L. G. Leal, J. Fluid Mech. **66**, 803 (1972).
[22] Y. L. Raikher, V. I. Stepanov, J.-C. Bacri, and R. Perzynski, Phys. Rev. E **66**, 021203 (2002).
[23] M. A. Martsenyuk, Y. L. Raikher, and M. I. Shliomis, Sov. Phys. JETP **38**, 413 (1974).
[24] H. P. Schwan and K. Foster, Proc. IEEE **68**, 104 (1980).
[25] R. Hergt and S. Dutz, J. Magn. Magn. Mater. **311**, 187 (2007).
[26] V. V. Murashov and G. N. Patey, J. Chem. Phys. **112**, 9828 (2000).